

# Shear stresses around circular cylindrical openings

P.C.J. Hoogenboom<sup>1</sup>, C. van Weelden<sup>1</sup>, C.B.M. Blom<sup>1,2</sup>

<sup>1</sup> Delft University of Technology, the Netherlands

<sup>2</sup> Gemeentewerken Rotterdam, the Netherlands

In this paper stress concentrations are studied around circular cylindrical openings or voids in a linear elastic continuum. The loading is such that a uniform shear stress occurs in the continuum, which is disturbed by the opening. The shear stress is in the direction of the centre axis of the opening. The stress distribution has been determined both analytically and numerically. It is shown that a peak shear stress occurs next to the opening. The peak shear stress is twice the shear stress at a large distance of the opening. In addition, a lining has been considered and formulas have been derived to calculate the stresses in the lining. The results are applied to a reinforced concrete bore tunnel in a soft soil. The soil is deformed in shear at the connection of the tunnel to a ventilation shaft. It is shown that large shear stresses can occur in the concrete due to minor differential settlements.

*Key words: Stress concentration, shear, cylindrical opening, cylindrical void, lining, tunnel, soft soil, reinforced concrete*

## 1 Introduction

The considered situation is shown in Figure 1. A cylindrical opening is enclosed by an infinite continuum. The continuum is loaded such that a uniform shear stress occurs, which is disturbed by the opening. The shear stress is in the direction of the opening axis. Around the opening stress concentrations occur which are analysed in this paper.

Stress concentrations around openings in solids and plates have been studied intensively. Many of the results are summarised by Savin (1961), Timoshenko et al. (1970), and Pilkey (1997). Stresses around cylindrical openings, representing tunnels, have been studied by Mindlin (1939) and Yu (1952). However, as far as the authors know, the situation considered in this paper has not been published before. This can be considered remarkable

because the analysis shows to be rather elementary and the result is quite relevant to civil engineering.

Stress concentration factors for normal stresses or shear stress in planes perpendicular to the centre line of the cylindrical opening are not considered in this paper. These can be simplified to two dimensional problems for which solutions are available in literature.<sup>1</sup>

## 2 Analytical solution

The derivation uses both cylinder coordinates  $x, r, \varphi$  and Cartesian coordinates  $x, y, z$  (Fig. 2). The reason for using two coordinate systems is that it is convenient to calculate the boundary stresses in cylinder coordinates and the far field stresses in Cartesian coordinates, as will be shown. The following displacement field is proposed

$$\begin{aligned} u_x &= \frac{\tau}{G} \left( r + \frac{a^2}{r} \right) \sin \varphi, \\ u_y &= 0, \\ u_z &= 0, \end{aligned} \tag{1}$$

The symbols  $a, r$  and  $\varphi$  are explained in Figure 2. Symbol  $G$  is the shear modulus and  $\tau$  is a parameter that will be interpreted below. It will be shown that this displacement field,

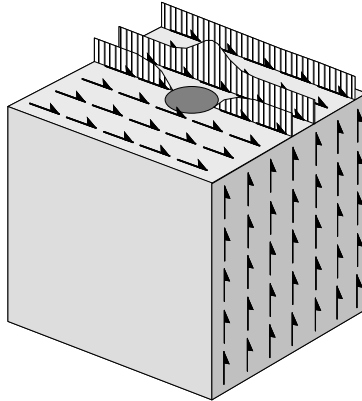


*Figure 1. Shear stress concentration in a continuum around a cylindrical opening*

---

<sup>1</sup> Most stress concentration problems for cylindrical openings can be simplified to a two dimensional plane strain problem or to a two dimensional plane stress problem. It is noted that plane strain problems have the same stress solutions as plane stress problems.

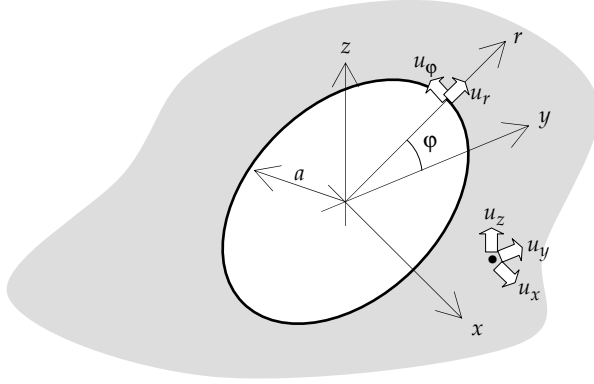


Figure 2. Reference systems, dimensions and displacements for the analytical solution

which has been found by trial and error, provides the correct solution to the problem of this paper. From Eq. (1) it follows that the displacements in the radial and tangential directions are

$$\begin{aligned} u_r &= 0, \\ u_\phi &= 0. \end{aligned} \quad (2)$$

The strains in cylindrical directions are

$$\begin{aligned} \epsilon_{xx} &= \epsilon_{rr} = \epsilon_{\phi\phi} = \gamma_{r\phi} = 0 \\ \gamma_{xr} &= \frac{\partial u_x}{\partial r} + \frac{\partial u_r}{\partial x} = \frac{\tau}{G} \left(1 - \frac{a^2}{r^2}\right) \sin \phi, \\ \gamma_{x\phi} &= \frac{\partial u_x}{r \partial \phi} + \frac{\partial u_\phi}{\partial x} = \frac{\tau}{G} \left(1 + \frac{a^2}{r^2}\right) \cos \phi. \end{aligned} \quad (3)$$

The stresses are

$$\begin{aligned} \sigma_{xx} &= \sigma_{rr} = \sigma_{\phi\phi} = \sigma_{r\phi} = 0 \\ \sigma_{xr} &= G \gamma_{xr}, \\ \sigma_{x\phi} &= G \gamma_{x\phi}. \end{aligned} \quad (4)$$

At the opening edge ( $r = a$ ) the stresses are

$$\begin{aligned} \sigma_{xx} &= \sigma_{rr} = \sigma_{\phi\phi} = \sigma_{r\phi} = 0 \\ \sigma_{xr} &= 0, \\ \sigma_{x\phi} &= 2\tau \cos \phi. \end{aligned} \quad (5)$$

In Cartesian coordinates  $u_x$  (Eq. 1) becomes  $u_x = \frac{\tau}{G}(1 + \frac{a^2}{y^2 + z^2})z$ . From this, the strains in the  $x, y, z$  directions can be derived.

$$\begin{aligned}\epsilon_{xx} &= \epsilon_{yy} = \epsilon_{zz} = \gamma_{yz} = 0, \\ \gamma_{xz} &= \frac{\partial u_x}{\partial z} + \frac{\partial u_z}{\partial x} = \frac{\tau}{G} \left( 1 + \frac{a^2(y^2 - z^2)}{(y^2 + z^2)^2} \right), \\ \gamma_{xy} &= \frac{\partial u_x}{\partial y} + \frac{\partial u_y}{\partial x} = -2 \frac{\tau}{G} \frac{a^2 y z}{(y^2 + z^2)^2}.\end{aligned}\tag{6a}$$

Since,  $\frac{y^2}{r^2} - \frac{z^2}{r^2} = \cos^2 \varphi - \sin^2 \varphi = \cos 2\varphi$  and  $2 \frac{z}{r} \frac{y}{r} = 2 \sin \varphi \cos \varphi = \sin 2\varphi$ , the shear strains  $\gamma_{xz}$  and  $\gamma_{xy}$  can be written as

$$\begin{aligned}\gamma_{xz} &= \frac{\tau}{G} \left( 1 + \frac{a^2}{r^2} \cos 2\varphi \right), \\ \gamma_{xy} &= -\frac{\tau}{G} \frac{a^2}{r^2} \sin 2\varphi.\end{aligned}\tag{6b}$$

The stresses are

$$\begin{aligned}\sigma_{xx} &= \sigma_{yy} = \sigma_{zz} = \sigma_{yz} = 0, \\ \sigma_{xz} &= G \gamma_{xz}, \\ \sigma_{xy} &= G \gamma_{xy}.\end{aligned}\tag{7}$$

The equilibrium equations are

$$\begin{aligned}\frac{\partial \sigma_{xx}}{\partial x} + \frac{\partial \sigma_{xy}}{\partial y} + \frac{\partial \sigma_{xz}}{\partial z} &= 0, \\ \frac{\partial \sigma_{xy}}{\partial x} + \frac{\partial \sigma_{yy}}{\partial y} + \frac{\partial \sigma_{yz}}{\partial z} &= 0, \\ \frac{\partial \sigma_{xz}}{\partial x} + \frac{\partial \sigma_{yz}}{\partial y} + \frac{\partial \sigma_{zz}}{\partial z} &= 0,\end{aligned}\tag{8}$$

which are correctly fulfilled. From Eq. (7) and (6b) follows that in the far field ( $r \rightarrow \infty$ ) the stresses are

$$\begin{aligned}\sigma_{xx} &= \sigma_{yy} = \sigma_{zz} = \sigma_{yz} = 0, \\ \sigma_{xz} &= \tau, \\ \sigma_{xy} &= 0.\end{aligned}\tag{9}$$

From Eq. (5) is concluded that the stresses on the opening edge are zero, which is the correct boundary condition. From Eq. 9 is concluded that  $\tau$  is a uniform shear stress in the continuum which is the correct loading. In addition, all equations of the linear theory of elasticity have been fulfilled. Therefore, the proposed displacement field Eq. (1) provides the correct solution to the problem of this paper.

The maximum shear stress occurs at  $(y = \pm a, z = 0)^2$

$$\begin{aligned}\sigma_{xz} &= 2\tau, \\ \sigma_{xy} &= 0.\end{aligned}\tag{10}$$

This follows from both Eq. (5) as Eq. (7).

### 3 Numerical solution

A finite element study has been performed using the program Ansys (Weelden 2010). The opening, with a radius of 2.5 m, is embedded in a square block of 50 x 50 x 50 m. Young's modulus  $E = 200000 \text{ N/mm}^2$  and Poisson's ratio  $\nu = 0.3$ . The element size is approximately 0.5 m close to the opening and larger at the block edges (Fig. 3). The element types used are SOLID45, which is an 8 node hexahedron and SOLID92 which is a 10 node tetrahedron. A shear displacement of 1 m is imposed to one of the block edges deforming it to a rhombic

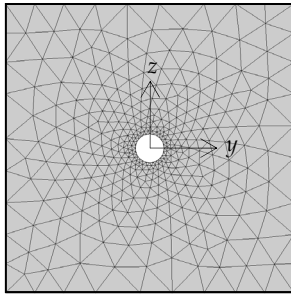


Figure 3. Tetrahedral finite element mesh of the front face

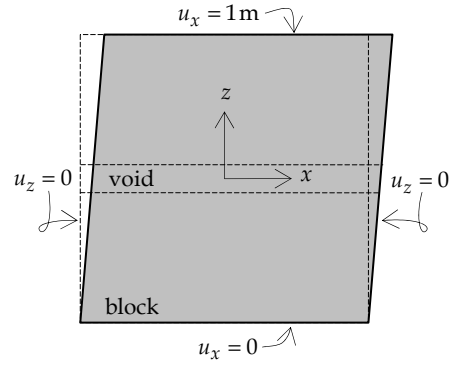


Figure 4. Imposed deformations on the model edges. In addition, one node is fixed in the  $y$  direction.

<sup>2</sup> This maximum shear stress of  $2\tau$  been suggested before by Hoogenboom et al. (2005).

shape (Fig. 4).<sup>3</sup> A static linear elastic analysis has been performed. The results show a shear stress next to the edges of the block of 1538 N/mm<sup>2</sup> (Fig. 5). The largest shear stress is 3102 N/mm<sup>2</sup>, which occurs in the middle of the block next to the opening. Therefore, the stress concentration factor is  $3102/1538 = 2.017$ . The analysis has been repeated for different values of Young's modulus, Poisson's ratio and the imposed deformation. This did not result in significant changes in the stress concentration factor. The analysis has been repeated for several element sizes. For a very fine finite element mesh the stress concentration factor is close to two. Also, the analysis has been repeated for several block sizes. For smaller block sizes both the concentrated stress and the stress in the block edges increase significantly.

In total 50 finite element analyses have been performed. The mean stress concentration factor is 1.996. The standard deviation is 0.017. The null hypothesis is, "the stress concentration factor is two". A 5% error is accepted in falsely rejecting the null hypothesis. The reliability boundaries are  $2 - 2.01 \times 0.017 / \sqrt{50} = 1.995$  and  $2 + 2.01 \times 0.017 / \sqrt{50} =$

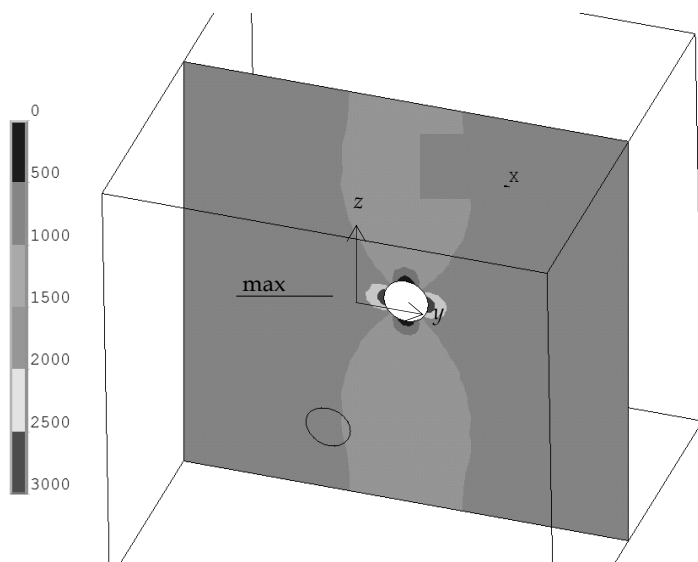


Figure 5. Shear stress  $\sigma_{xz}$  in the middle section of the block

---

<sup>3</sup> In retrospect, a 1 m slice of the block could have been analysed if a continuity condition would have been imposed on the boundaries  $x = 0.5$  m and  $x = -0.5$  m. This would enable the use of meshes of prismatic elements with unity lengths.

2.005, where 2.01 is 2.5% critical value of the Student distribution of 49 degrees of freedom. Since  $1.995 < 1.996 < 2.005$  the null hypothesis cannot be rejected.

#### 4 Lining stresses

A lining is introduced that covers the surface of the opening (Fig. 6). It has a thickness  $t$  and a shear stiffness  $G_l t$ . The shear deformation  $\gamma$  of the lining is the same as that of the continuum edge.

$$\gamma = \gamma_{x\varphi}(r = a, \varphi) . \quad (11)$$

The constitutive equation of the lining is

$$n = G_l t \gamma , \quad (12)$$

where  $n$  is the lining distributed shear force (N/m) in a cross-section of the opening. The lining is loaded by the shear stress  $\sigma_{xr}$  at the continuum edge. It is assumed that normal stresses do not occur in the lining, which hereafter is shown to be true.<sup>4</sup> The lining equilibrium equation is (Fig. 6)

$$(n + dn)dx - n dx + \sigma_{xr} a d\varphi dx = 0 .$$

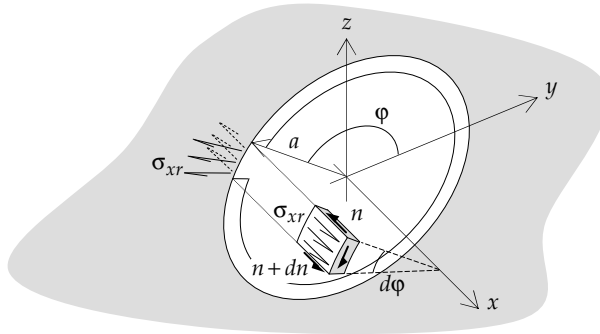


Figure 6. Equilibrium of an elementary part of the lining

<sup>4</sup> Problems in elasticity theory have a solution and just one solution (existence and uniqueness). Therefore, when a solution is found that fulfills all equations than this solution is the solution. The fact that some stresses are assumed to be zero is not an approximation but just part of the solution.

This can be evaluated to

$$\frac{dn}{d\varphi} + a\sigma_{xr}(r=a, \varphi) = 0 . \quad (13)$$

The following displacement field is proposed

$$\begin{aligned} u_x &= \frac{\tau}{G} \left( r + \frac{1-k}{1+k} \frac{a^2}{r} \right) \sin \varphi , \\ u_y &= 0 , \\ u_z &= 0 , \end{aligned} \quad (14)$$

where  $k$  is a parameter that is interpreted below. It is noted that when  $k = 0$  the displacement is equal to that of the previous chapter. It will be shown that Eq. (14), which has been found by trial and error, provides the correct solution to the problem of this paper including a lining.

It can be shown that for this displacement field the equilibrium conditions, Eq. (8), are fulfilled too. Also the far field conditions, Eq. (9), are fulfilled. The shear strains in the radial and tangential directions are

$$\begin{aligned} \gamma_{xr} &= \frac{\partial u_x}{\partial r} + \frac{\partial u_r}{\partial x} = \frac{\tau}{G} \left( 1 - \frac{1-k}{1+k} \frac{a^2}{r^2} \right) \sin \varphi , \\ \gamma_{x\varphi} &= \frac{\partial u_x}{r\partial\varphi} + \frac{\partial u_\varphi}{\partial x} = \frac{\tau}{G} \left( 1 + \frac{1-k}{1+k} \frac{a^2}{r^2} \right) \cos \varphi . \end{aligned} \quad (15)$$

In the continuum edge ( $r = a$ ) the shear stresses are

$$\begin{aligned} \sigma_{xr} &= \tau \frac{2k}{1+k} \sin \varphi , \\ \sigma_{x\varphi} &= \tau \frac{2}{1+k} \cos \varphi . \end{aligned} \quad (16)$$

Substitution of Eq. (11) and (15) in Eq. (12) gives

$$n = \tau \frac{G_I t}{G} \frac{2}{1+k} \cos \varphi . \quad (17)$$

Substitution of Eq. (17) and (16) in Eq. (13) and evaluation gives

$$k = \frac{G_I t}{G a} . \quad (18)$$



Apparently,  $k$  is a dimensionless parameter that describes the stiffness properties of the lining compared to the continuum. With this result, all equations of the continuum and the lining are fulfilled. Also, the far field stress state (Eq. 9) is fulfilled. Also, compatibility (Eq. 11) and equilibrium (Eq. 13) between the continuum and the lining are fulfilled. Therefore, the proposed displacement field Eq. (14) provides the correct solution to the problem of this paper including a lining.

The resulting shear stress in the edge of the continuum can be obtained from Eq. (16)

$$\sqrt{\sigma_{xr}^2 + \sigma_{xz}^2} = \tau \frac{2}{1+k} \sqrt{k^2 \sin^2 \varphi + \cos^2 \varphi}. \quad (19)$$

For  $0 \leq k < 1$  the extreme value is

$$\tau_{\max} = \tau \frac{2}{1+k}, \quad (20)$$

which occurs at  $\varphi = 0$ . For  $k = 1$  there is no extreme value because there is no disturbance in the continuum stress field. For  $k > 1$  the extreme value is

$$\tau_{\max} = \tau \frac{2k}{1+k}, \quad (21)$$

which occurs at  $\varphi = \pm \frac{1}{2} \pi$ . This result is shown in Figures 7 and 8.

From Eq. (17) and (18) the maximum shear stress in the lining is obtained

$$\frac{n}{t} = \tau \frac{a}{t} \frac{2k}{1+k}, \quad (22)$$

which occurs at  $\varphi = 0$  for any  $k$ .

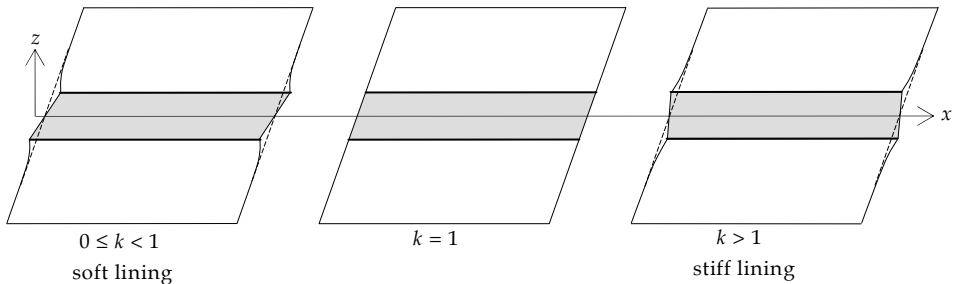


Figure 7. Continuum and lining deformation for three types of stiffness  $k$

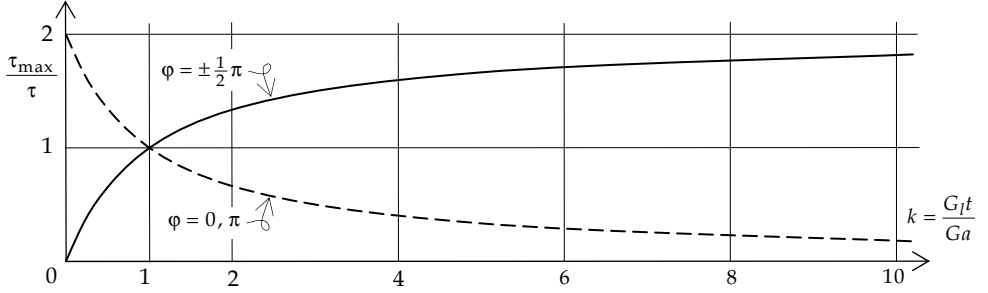


Figure 8. Stress concentration factor  $\frac{\tau_{\max}}{\tau}$  in the continuum as function of the lining stiffness  $k$

It can be practical to express  $k$  in Young's modulus  $E_l$  of the lining and Young's modulus  $E$  of the continuum, provided that Poisson's ratio of lining and soil are the same.

$$k = \frac{E_l t}{E a} \quad (23)$$

## 5 Tunnel stresses

Bore tunnels in soft soils often have reinforced concrete linings with a thickness of approximately radius/10. The lining typically consists of connected concrete segments. Young's modulus of concrete including the connections is approximately 10000 N/mm<sup>2</sup>. The stiffness of soil strongly depends on the confinement pressure. At a depth of 10 m soil can be modelled as an elastic continuum with Young's modulus 100 N/mm<sup>2</sup>. Consequently, the stiffness parameter  $k$  can be calculated by (Eq. 23).

$$k = \frac{E_l t}{E a} = \frac{10000 a/10}{100 a} = 10$$

At regular intervals a tunnel is interrupted by vertical ventilation shafts. A shaft is loaded differently than the tunnel parts. Also, the shaft foundation is in different soil layers than the tunnel. Consequently, shaft and tunnel experience different settlements (Fig. 9). This situation can be modelled by the problem that is solved in this paper. The soil deformation is approximated with a homogeneous shear strain. Due to this a homogeneous shear stress  $\tau$  occurs which is disturbed by the tunnel.

The maximum shear stress in the soil is (Eq. 21)

$$\tau_{\max} = \tau \frac{2k}{1+k} = \tau \frac{2 \times 10}{1+10} = 1.8 \tau .$$

which occurs next to the top and bottom of the tunnel lining. The maximum shear stress in the concrete lining is (Eq. 22)

$$\frac{n}{t} = \tau \frac{a}{t} \frac{2k}{1+k} = \tau \frac{a}{a/10} \frac{2 \times 10}{1+10} = 18 \tau .$$

This is a considerable stress concentration. It is noted that often the soil and concrete properties cannot be determined accurately. Fortunately, large variations in  $k$  have little influence on the results of this chapter. For example if  $k = 2$ , which is only 20% of the previous value then the concrete lining stress is  $n/t = 13.3 \tau$ , which is still 73% of the previous value.

Clearly, both the soil and the reinforced concrete tunnel segments behave nonlinearly, which is not included in the above linear analysis. Self weight and the construction process cause stresses in the soil and the lining. In addition, the settlement considered in this paper can occur. The soil can yield at the connection with the tunnel which might unload the concrete. Nevertheless, the present linear analysis of the additional settlement load predicts that before yielding the maximum additional concrete stresses are ten times larger than the maximum of the additional soil stresses. It is not unlikely that the already heavily loaded concrete crushes before the soil yields. More research is needed for validation of this conclusion.

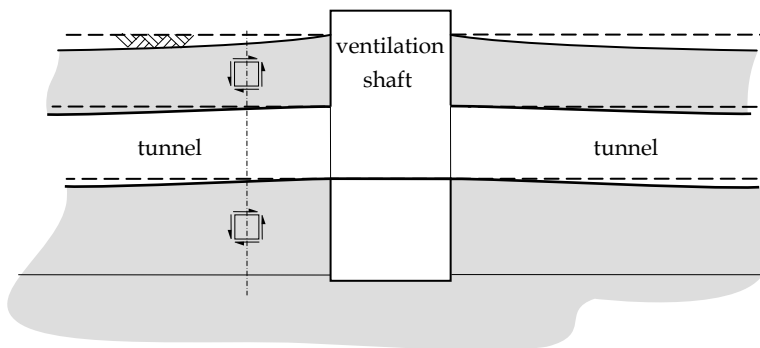


Figure 9. Differential settlements around a bore tunnel connected to a ventilation shaft

## 6 Conclusions

A factor two stress concentration occurs in a continuum with a circular cylindrical opening loaded in shear in the direction of the opening centre line. This result does not depend on the opening diameter or on Young's modulus. Contrary to spherical openings this stress concentration does not depend on Poisson's ratio.

Also for cylindrical openings with a lining, closed form solutions have been derived for the stress concentration in the continuum and in the lining. The stress concentration factor for the continuum varies between one and two depending on the lining stiffness.

Application to a typical bore tunnel in soft soil with a reinforced concrete lining shows that small differential settlements causing small shear stresses in the soil can give large shear stresses in the lining. The shear stress in the concrete lining can be as much as 18 times larger than the shear stress in the soil at some distance of the tunnel.

## Literature

- Calladine C.R. (1983) *"Theory of shell structures"*, Cambridge University Press
- Hoogenboom P.C.J., Spaan R. (2005) "Shear Stiffness and Maximum Shear Stress of Round Tubular Members", *15th International Offshore and Polar Engineering Conference (ISOPE-2005)*, Seoul, June 19-24, 2005, Vol. 4, pp. 316-319
- Mindlin R.D. (1939) "Stress distribution around a tunnel", *Proceedings of the American Society of Civil Engineers*, Vol. 65, No. 4, pp. 619-642
- Pilkey W.D., Pilkey D.F. (2008) *"Peterson's stress concentration factors"*, Third edition, John Wiley & Sons, New York
- Savin G.N. (1961) *"Stress concentrations around holes"*, Translated from Russian by Gros and Johnson, Pergamon Press, Oxford
- Timoshenko S.P., Goodier J.N. (1970) *"Theory of Elasticity"*, third edition, McGraw-Hill book company, Singapore
- Weelden C. van (2010) *"Schuifspanningen loodrecht op een cilindrisch gat"*, Bachelor report, Delft University of Technology (In Dutch), online: [http://www.mechanics.citg.tudelft.nl/~pierre/BSc\\_projects/BSc\\_projects.html/eindrapport\\_van\\_weelden.pdf](http://www.mechanics.citg.tudelft.nl/~pierre/BSc_projects/BSc_projects.html/eindrapport_van_weelden.pdf)
- Yu Y.Y. (1952) "Gravitational stresses on deep tunnels", *Transactions of the American Society of Mechanical Engineers, Applied Mechanics Section*, Vol. 74, pp. 537.

## Notation

$a$ .....	opening diameter
$E$ .....	Young's modulus of the continuum
$E_l$ .....	Young's modulus of the lining
$G$ .....	shear modulus of the continuum
$G_l$ .....	shear modulus of the lining
$k$ .....	dimensionless stiffness factor of the lining
$n$ .....	in plane shear force per unit length in the lining
$r$ .....	radial coordinate (Fig. 2)
$t$ .....	lining thickness
$u_x, u_y, u_z$ .....	displacements of a continuum point (Fig. 2)
$u_r, u_\phi$ .....	displacements of a continuum point in cylinder coordinates (Fig. 2)
$\epsilon_{xx}, \epsilon_{yy}, \epsilon_{zz}$ .....	normal strains of a continuum point
$\phi$ .....	angle coordinate (Fig. 2)
$\gamma$ .....	shear strain in the lining
$\gamma_{xy}, \gamma_{xz}, \gamma_{yz}$ .....	shear strains of a continuum point
$\gamma_{xr}, \gamma_{x\phi}$ .....	shear strains of a continuum point in cylinder coordinates
$\sigma_{xx}, \sigma_{yy}, \sigma_{zz}$ .....	normal stresses of a continuum point
$\sigma_{xy}, \sigma_{xz}, \sigma_{yz}$ .....	shear stresses of a continuum point
$\sigma_{xr}, \sigma_{x\phi}$ .....	shear stresses of a continuum point in cylinder coordinates
$\tau$ .....	far field shear stress in the continuum
$\tau_{\max}$ .....	peak stress in the continuum

## Appendix

In this appendix is shown that Eq. (13) can also be derived from the membrane theory of thin shells. For this a new reference system  $x, y, z$  is selected in the middle surface of the tunnel lining (Fig. 10). This reference system follows the lining such that the new  $z$ -axis is always perpendicular to the lining. The equilibrium equations for membrane forces in thin shells are, Calladine (1983)

$$\begin{aligned} k_x n_{xx} + k_y n_{yy} + 2k_{xy} n_{xy} + p_z &= 0 \\ n_{xx,x} + n_{xy,y} + p_x &= 0 \\ n_{yy,y} + n_{xy,x} + p_y &= 0 \end{aligned} \quad (24)$$

In which the factors  $k$  are the shell curvatures and the terms  $p$  are the shell loading. For the lining  $k_x = -1/a$ ,  $k_y = 0$ ,  $k_{xy} = 0$ ,  $p_x = \sigma_{r\varphi}(r = a, \varphi)$ ,  $p_y = \sigma_{xr}(r = a, \varphi)$  and  $p_z = \sigma_{rr}(r = a, \varphi)$ . In the notation of this paper the lining shear force is  $n$ , therefore,  $n_{xy} = n$ . In addition,  $n_{yy} = n_{xx}$ ,  $n_{xx} = n_{\varphi\varphi}$ . Subsequently, Eq. (24) can be written as

$$\begin{aligned} -\frac{n_{xx}}{a} + \sigma_{rr}(r = a, \varphi) &= 0 \\ \frac{\partial n_{\varphi\varphi}}{\partial \varphi} + \frac{\partial n}{\partial x} + \sigma_{r\varphi}(r = a, \varphi) &= 0 \\ \frac{\partial n_{xx}}{\partial x} + \frac{\partial n}{\partial \varphi} + \sigma_{xr}(r = a, \varphi) &= 0 \end{aligned} \quad (25)$$

Since, all derivatives to  $x$  are zero, the last line of Eq. (25) can be written as

$$\frac{dn}{d\varphi} + a\sigma_{xr}(r = a, \varphi) = 0 ,$$

which was to be proven.

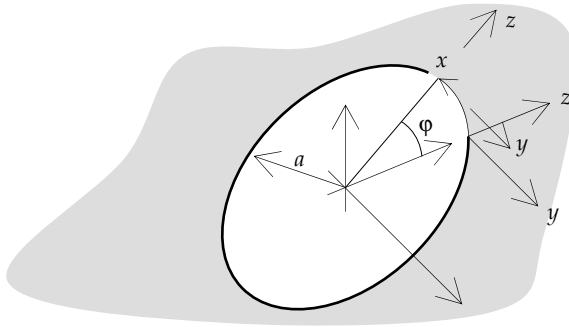


Figure 10. Reference system of the shell equilibrium equations